Electronic Supplementary Material (ESI) for Physical Chemistry Chemical Physics.

Supporting information

for

Insights into the limitations of solar cells sensitized with ruthenium dyes revealed in time-resolved spectroscopy studies

Mateusz Gierszewski [1], Iwona Grądzka [1], Adam Glinka [1], and Marcin Ziółek[1] *

[1] *Quantum Electronics Laboratory, Faculty of Physics, Adam Mickiewicz University in Poznań, Umultowska 85, 61-614 Poznań, Poland.*

* corresponding author, email: marziol@amu.edu.pl

Table S1A. Number of measured samples (N) and relative errors of the calculated averaged photovoltaic parameters (given in Table 1) for the studied solar cells. The relative error of parameter p is defined as the standard deviation of the mean (Δp) divided by the mean value (from Table 1) and multiplied by 100 %.

Cell	N	$\frac{\Delta V_{OC}}{\overline{V_{OC}}}$ [%]	$\frac{\Delta FF}{\overline{FF}}$ [%]	$\frac{\Delta J_{SC}}{\overline{J_{SC}}}$ [%]	$\frac{\Delta Eff}{\overline{Eff}}$ [%]
I_1	6	0.4	1.4	4.3	3.8
I_2	6	0.4	1.5	2.3	0.8
I_2_lowTi	6	0.5	1.0	1.7	1.6
I_3	6	0.4	4.7	4.1	2.3
Co_1_ lowTi	4	0.6	1.3	4.1	3.9
Co_2_ lowTi	6	0.3	3.4	2.7	5.1
Co_2	6	0.8	1.2	2.8	1.2
Co_3_ lowTi	4	0.6	1.5	1.6	2.2
I_2_s	6	0.8	2.3	4.3	2.3
I_2_s_lowTBP	4	0.8	1.4	2.3	1.7
I_3_s	6	0.5	2.8	1.3	2.0
I_3_s_lowTBP	4	0.6	10.9	2.4	9.2

Table S1B. Photovoltaic parameters of the best solar cells sensitized by N719+CDCA of each configuration: open circuit voltage (V_{OC}), fill factor (*FF*), photocurrent density (J_{SC}), efficiency (*Eff*) number of absorbed photons at 1Sun illumination (N_{ph}), absorbance at 500 nm ($A_{500\ nm}$) and corrected photocurrent efficiency (*Total APCE*).

Cell	V_{OC} [V]	*FF*	J_{SC} [mAcm^{-2}]	*Eff* [%]	N_{ph} [10^{20} s^{-1}m^{-2}]	$A_{500\ nm}$	*Total APCE*
I_1	0.79	0.67	8.3	4.4	6.6	0.54	0.78
I_2	0.76	0.59	11.9	5.3	8.0	0.75	0.92
I_2_lowTi	0.79	0.66	10.0	5.3	7.4	0.64	0.84
I_3	0.76	0.56	13.4	5.8	9.0	1.03	0.94
Co_1_ lowTi	0.73	0.57	4.6	1.9	5.3	0.38	0.54
Co_2_ lowTi	0.72	0.51	6.0	2.2	6.9	0.57	0.54
Co_2	0.71	0.56	6.5	2.5	8.0	0.75	0.50
Co_3_ lowTi	0.69	0.47	7.0	2.3	8.8	0.94	0.49
I_2_s	0.81	0.57	12.1	5.5	8.8	0.96	0.86
I_2_s_lowTBP	0.76	0.59	11.9	5.4	8.8	0.96	0.84
I_3_s	0.79	0.53	14.3	6.0	11.1	1.74	0.80
I_3_s_lowTBP	0.74	0.36	15.4	4.2	11.1	1.74	0.86

A:

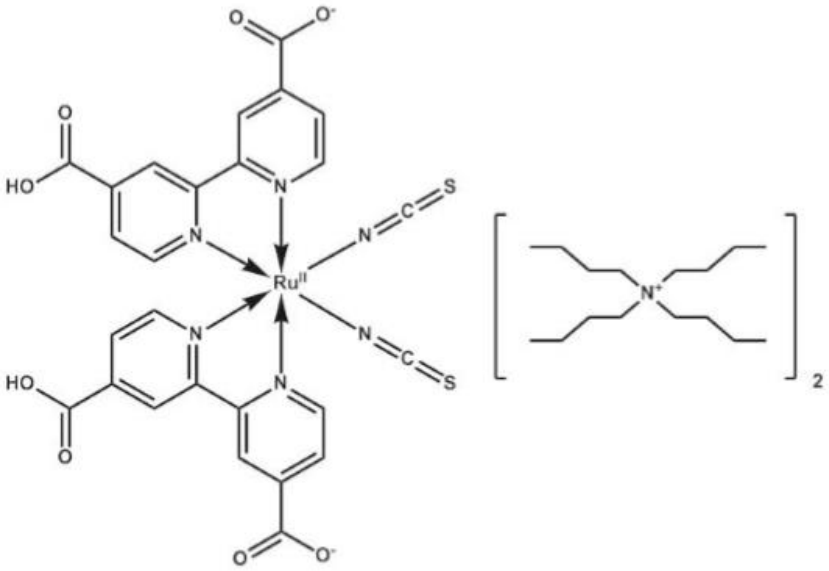

B:

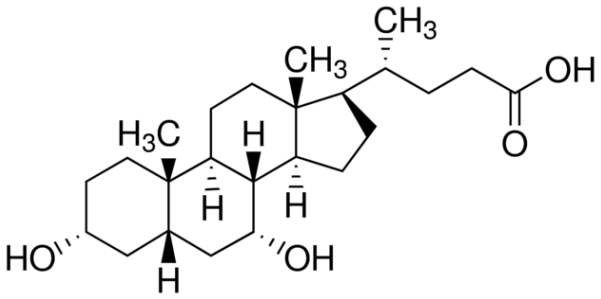

Scheme S1. The structure of N719 dye (A) and chenodeoxycholic acid, CDCA (B).

A:

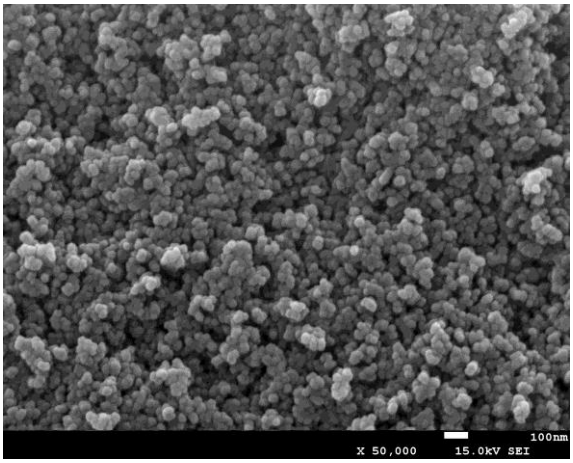

B:

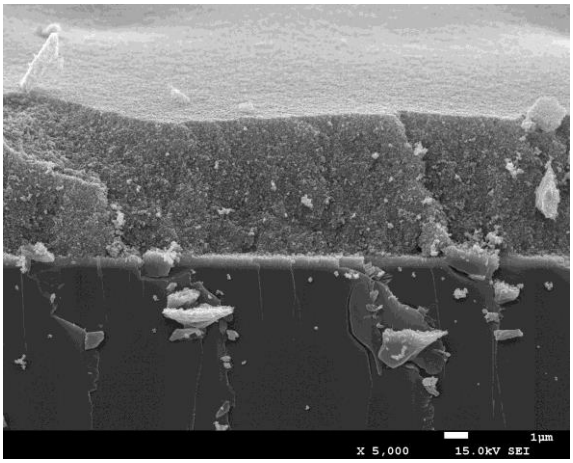

C:

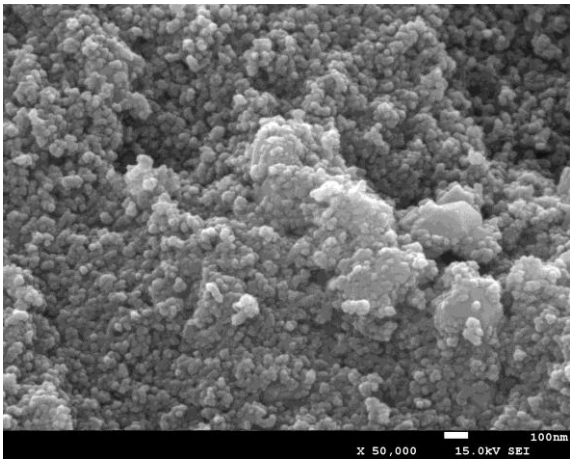

D:

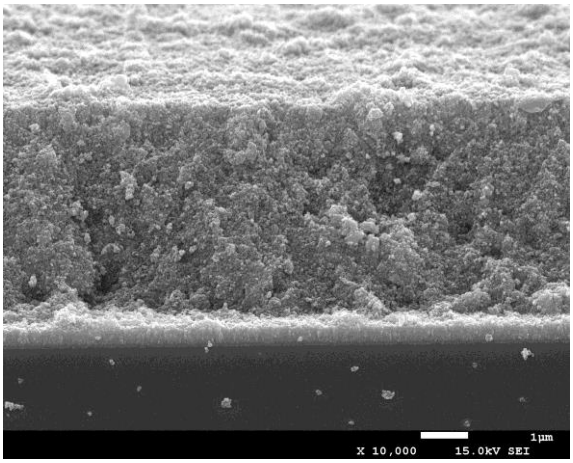

E:

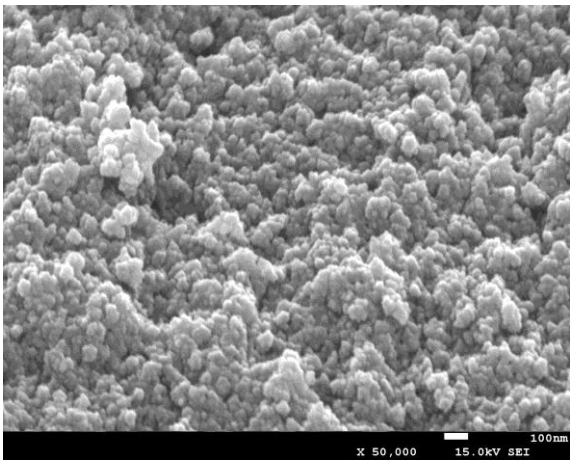

F:

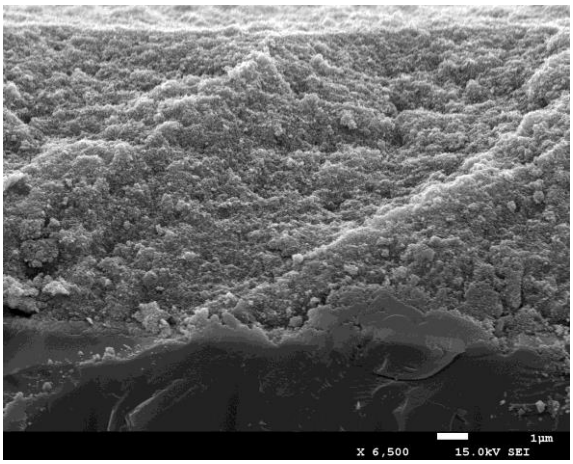

Figure S1. SEM cross-sections images for **I_2_lowTi** (A-B) **I_2_s** (C-D), **I_2** (E), **I_3_s** (F)

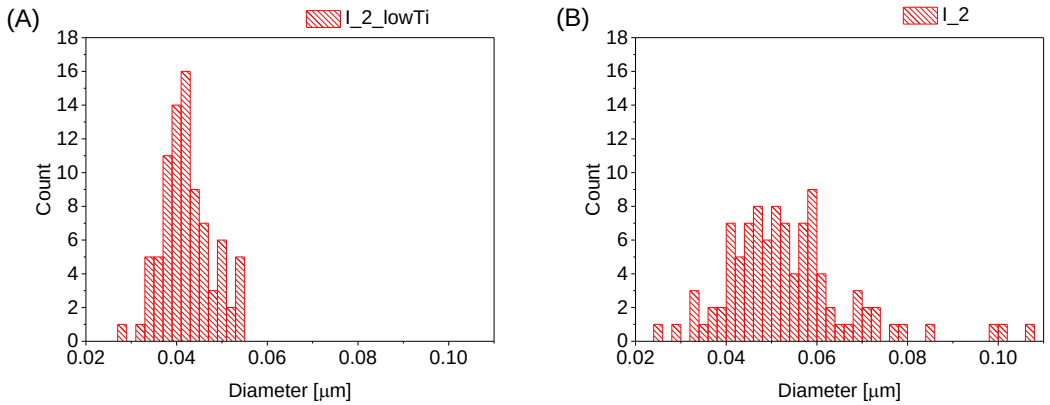

Figure S2. Analysis of nanoparticle diameter distribution after 20 mM $TiCl_4$ (I_2_lowTi, A) and 50 mM (I_2, B) post-treatment

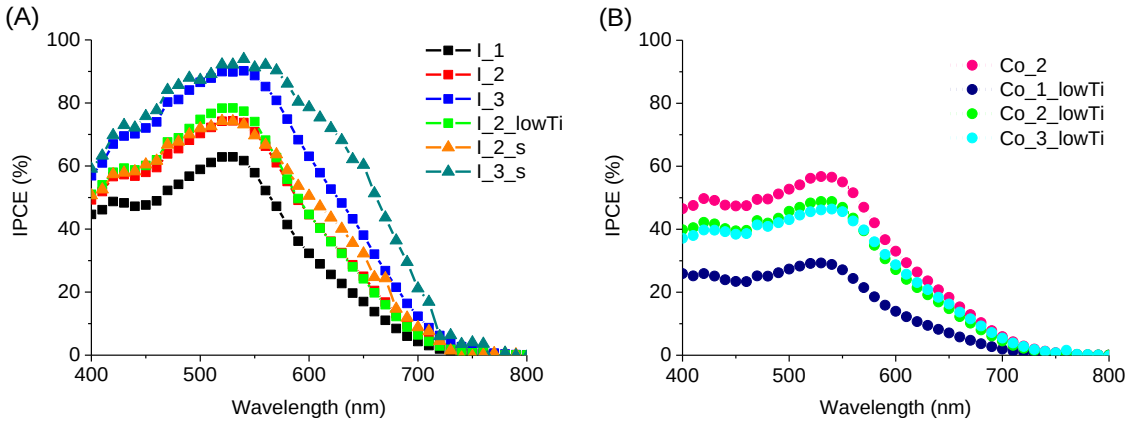

Figure S3. IPCE spectra of selected cells sensitized with N719+CDCA in the different, indicated configurations; iodide (A) and Co-Bpy (B) electrolyte

A:

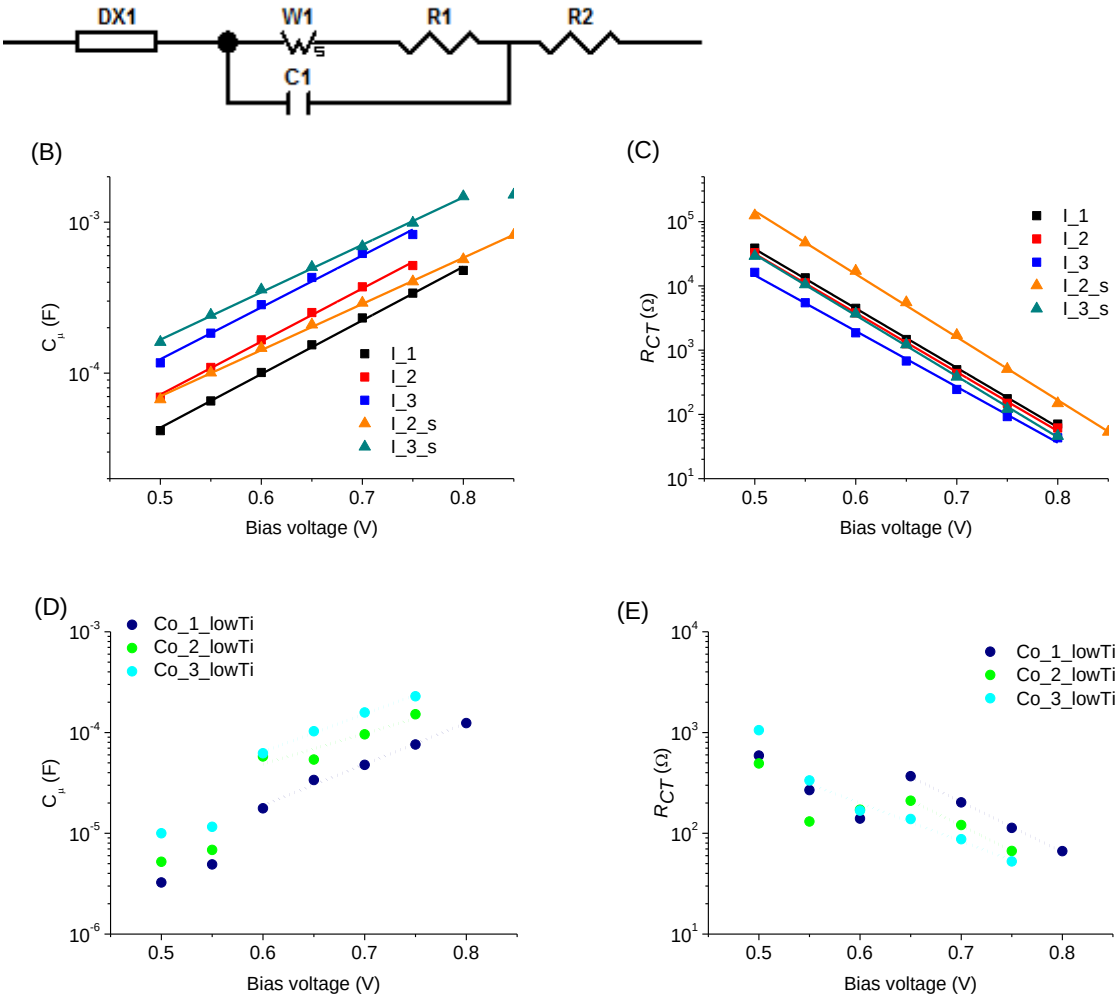

Figure S4. (A) Equivalent circuits for DSSCs based on N719 dye, DX1 is transmission line element. Chemical capacitance (B, D) and charge transfer resistance (C, E) of different cells sensitized by N719+CDCA in different cell configurations using iodide (B-C) and Co-Bpy (D-E) electrolyte.

Table S2. Calculated ideality factor (*m*) and trap distribution parameter (α) for obtained cells sensitized by N719+CDCA in different configurations. The parameters α and *m* were obtained from the fit (Figure S3) of the following functions: $C_\mu = C_0 \exp(\alpha\, Ve/kT)$ and $R_{ct} = R_0 \exp(-Ve/m\, kT)$.

Sample / configuration	*m*	α
I_1	1.8	0.21
I_2	1.8	0.21
I_2_lowTi	1.8	0.19
I_3	2.0	0.20
Co_1_lowTi	3.4	0.24
Co_2	2.5	0.20
Co_2_lowTi	3.4	0.18
Co_3_lowTi	4.5	0.24
I_2_s	1.7	0.18
I_2_s_lowTBP	1.7	0.18
I_3_s	1.8	0.18
I_3_s_lowTBP	2.0	0.17

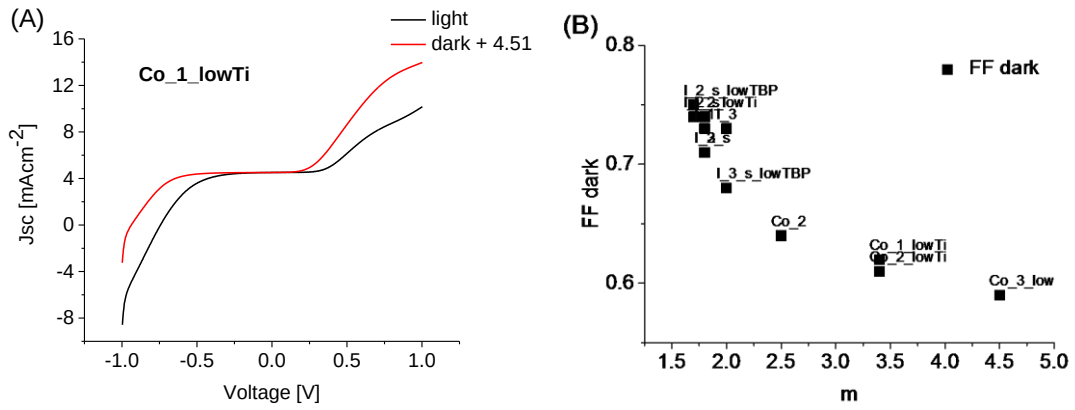

Figure S5. C-V curves measured at 1Sun illumination and simulated ideal C-V curves for **Co_1_lowTi** (A); the simulated ideal C-V curves obtained adding J_{SC} to dark C-V curves of the cell. (B) Plot of *FF* (from the C-V curves at the dark conditions) as a function of ideality factor *m* (from EIS measurements).

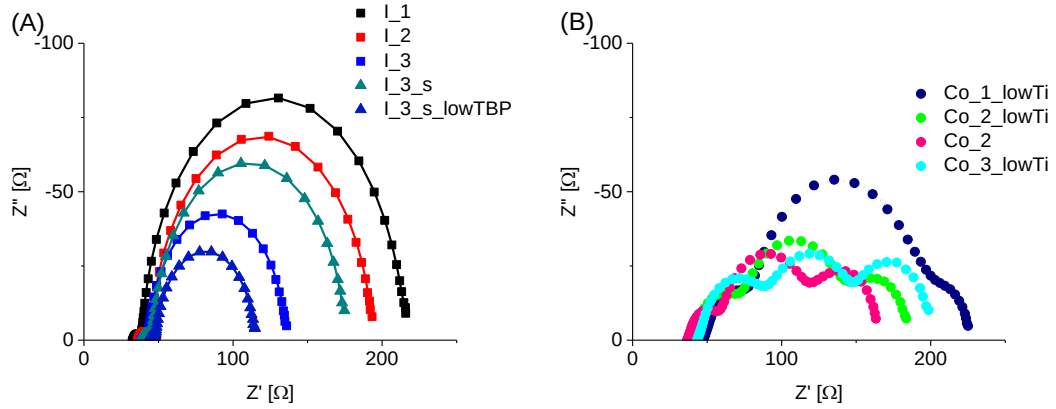

Figure S6. Nyquist plots for different cells sensitized by N719+CDCA in different configurations with iodide (A) and Co-Bpy electrolyte (B).

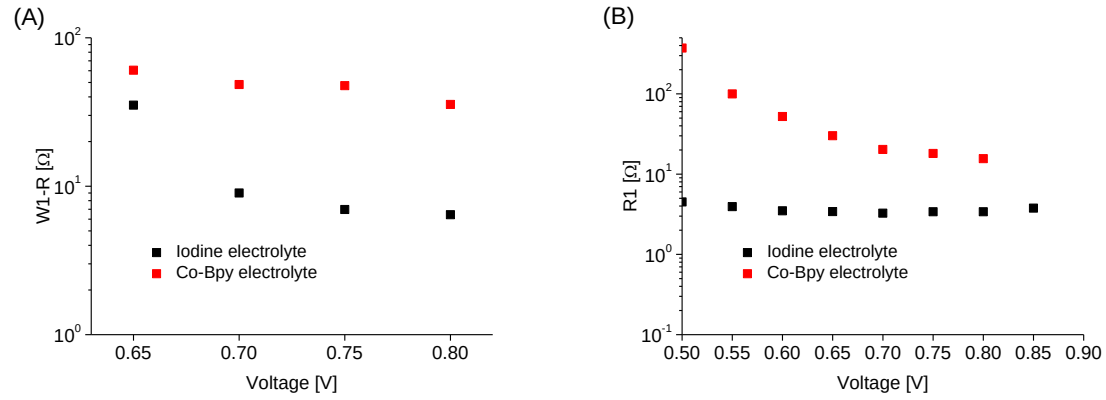

Figure S7. Averaged values of Warburg resistance (W1_R, Figure A) and the counter electrode/electrolyte interface resistance (R1, Figure B) for different cells sensitized by N719+CDCA in different configurations with iodide and Co-Bpy electrolyte.

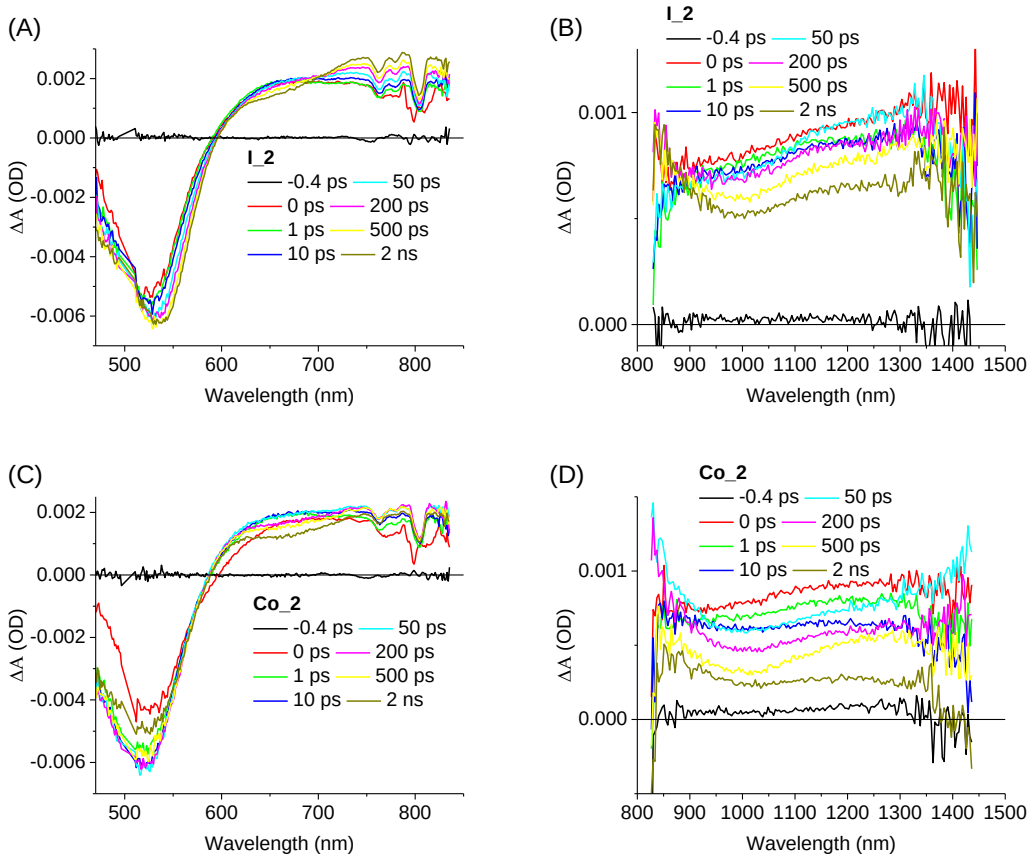

Figure S8. Exemplary transient spectra for selected delay time between pump and probe pulses for **I_2** and **Co_2** in both VIS (A, C) and NIR (B, D) ranges.

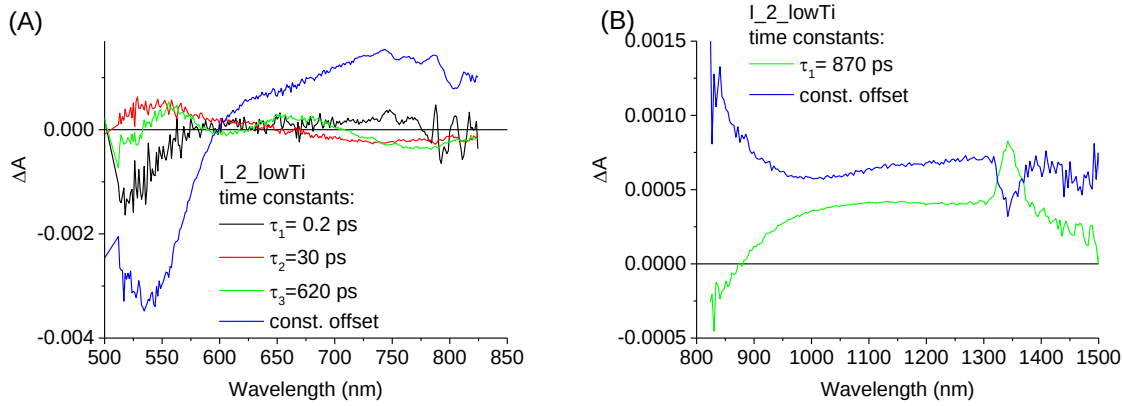

Figure S9. Wavelength dependent amplitudes of the indicated time constants obtained from global analysis (three or one exponential with constant offset) of transient absorption spectra for DSSCs with iodide electrolyte (**I_2_lowTi**) in the VIS (A) and NIR (B) spectral ranges. The concentration of $TiCl_4$ was 20 mM (compare with Figure 4C-D).

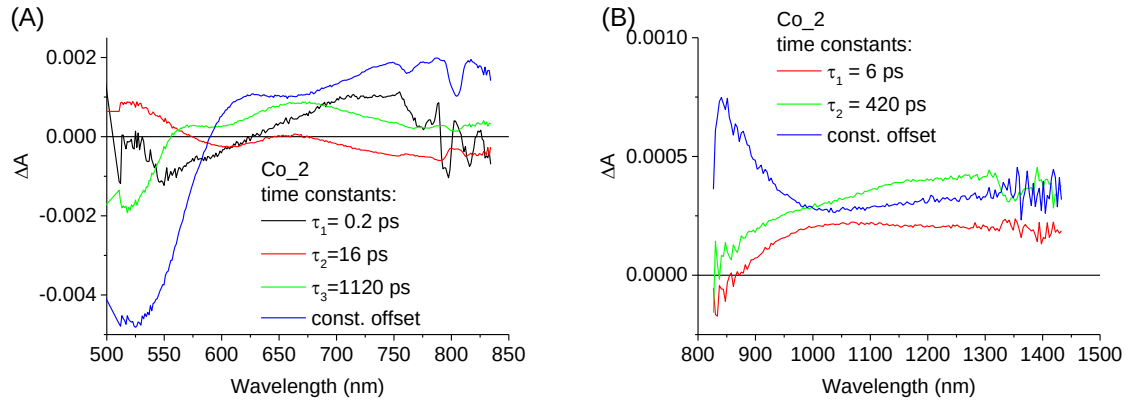

Figure S10. Wavelength dependent amplitudes of the indicated time constants obtained from global analysis (three or one exponential with constant offset) of transient absorption spectra for DSSCs with cobalt electrolyte **Co_2** in the VIS (A) and NIR (B) spectral ranges. The concentration of $TiCl_4$ was 50 mM (compare with Figure 5C-D).

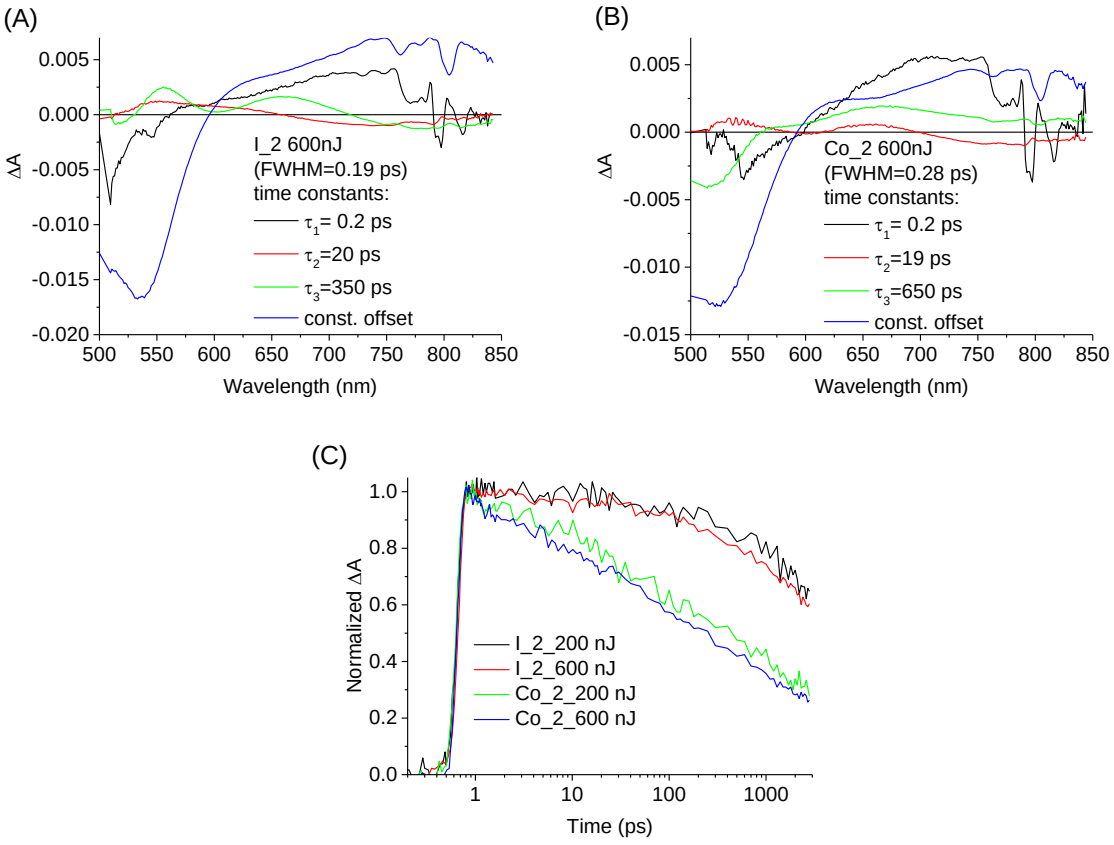

Figure S11. Pump energy effect in transient absorption studies. Wavelength dependent amplitudes of the indicated time constants obtained from global analysis of transient absorption spectra of I_2 sample (A) and Co_2 sample (B) in the VIS spectral range upon excitation with 600 nJ pump pulse (compare with Figures 4C and S10A). Kinetics at 1200 nm for selected iodide and cobalt cells under different pump pulse intensity (C).